A Theoretical Investigation of Decorated Novel
1,2-Di(4-pyridyl)-ethylene based Dye Sensitized Solar Cells (DSSC)

S. Krishnaveni[1,], X. Mary Josephine[2,], S. Mohankumar[3,] and V. Sathyanarayanamoorthi[1,*,]

[1]Department of Physics, PSG College of Arts and Science, Coimbatore-641014, India
[2]Department of Physics, Nirmala College for Women, Coimbatore-641018, India
[3]Department of Electronics, PSG College of Arts and Science, Coimbatore-641014, India

*Corresponding author: E-mail: sathyanarayanamoorthi@psgcas.ac.in

Density functional theory (DFT) approaches are employed to investigate the performance of dyes and the influence of p-conjugation in dye-sensitized solar cells (DSSCs). In this investigation, five new 1,2-di(4-pyridyl)-ethylene based conjugated donor-π-acceptor organic dyes (D-π-A) exist. The spacer is a diphenylamine (DPA) group, while the diphenyl amine group serves as the component that donates electrons in each system, the nitro/cyano group is used as an electron accepting group. An alternate methyl/ethyl group is employed as π-conjugated spacer in order to study the effect of the auxiliary donor group. Through performing DFT calculations with the B3LYP both the polarized split-valence 6-311++G (d,p) basis sets, an excitation energies, absorption spectra and emission spectra of each molecule were examined. The polarizable continuum model (PCM) is utilized in studying these impact for solvent. The energies at which these dyes are LUMO and HOMO, which assure the favourable impact for electron injection and these dye regeneration process. The calculation of the HOMO-LUMO gap demonstrates good agreement when compared to spectral information. The light-harvesting efficiency (LHE), electron injection free energy (ΔG^{inject}), as well as oscillator strength (f) are computed and explained. The calculated open-circuit photovoltage values (V_{oc}) and electron coupling constant (V_{RP}) for the studied dye-sensitizers are also included in this study.

Keywords: 1,2-Di(4-pyridyl)ethylene derivatives, Dye sensitized solar cells, Density functional theory, Light harvesting efficiency.

INTRODUCTION

Solar provides most accessible, endless, silent and suitable to large applications of all the renewable energy sources [1,2]. Solar radiation totals 3.8 million EJ annually, which consumes roughly 10,000 times as much energy as is now needed [3]. The application of photovoltaic systems directly converting solar energy into electrical energy without pollution, sound or moving parts would be desirable using the perspectives of environmental preservation and energy efficiency. This would make this dependable and long-lasting. Photovoltaic (PV) is an effective method that makes use of the sun's energy [4,5]. Traditional silicon-based solar cells are not suitable for home or other commercial applications due to their high cost and complex manufacturing process. However, a number of organic solar cells developed recently that bring together low module cost with the adaptability and lightweight nature of organic

molecules [6,7]. One of the most effective and reasonably priced silicon solar cell substitutes is the dye-sensitized solar cell. In 1991, O'regan & Gratzel [8] prepared the initial dye-sensitized nanocrystalline solar cells, whose incoming photon to electrical current efficiency for conversion was near to 80% and whose rate of photoelectric energy conversion was 7.1%. The efficiency of dye-sensitized solar cells has reached approximately 12% [9], a level that is considered commercially significant [10,11]. The simplicity of their structure and the affordability of this technology have also generated significant attention.

A wide range of coordination polymers (CPs) and metal-organic frameworks (MOFs) have been synthesized utilizing 1,2-di(4-pyridyl)ethylene as a major ligand or linker [12,13]. Cadmium-based coordination polymers (CPs) with pillared layers [14] are utilized to create expandable and contractible structures [15]. These structures incorporate a zinc dinuclear compound that exhibits luminescence when subjected to

controlled lighting conditions [16]. Additionally, self-assembly driven by multicomponent cooperation is employed to fabricate 3D tetragonal prisms composed of platinum [17]. Considering the spectroscopic characteristics of the existence of metal ions and ligands, MOFs and coordination polymers containing lanthanide [18-23] exhibit exciting photoluminescence capabilities. In order to achieve efficient luminescence of Ln^{3+} ions, it is necessary to prevent low light absorption coefficients associated with $4f$-$4f$ transitions, which can be accomplished by using organic light-harvesting compounds with high absorption coefficients. The sensitization of lanthanide ions is facilitated by the transfer of excitation energy between the ligand and the metal center, which can be achieved by the utilization of a suitable chemical linker [24]. The power location between the singlet and triplet states of the ligand [25] in the coordination polymer [26-29] determines whether a sensitization is effective. In order to develop coordination polymers with functional photoluminescence, a linker known as 1,2-di-(4-pyridyl)ethylene (DPY) has qualities that consists of both structural and electrical characteristics [30]. A 1,2-di-(4-pyridyl)ethylene solution in glacial acetic acid is used as another technique for sampling and analyzing atmospheric ozone. The 1,2-di-(4-pyridyl)-ethylene and collected ozone react for make an ozonide, which is then broken down to obtain pyridine-4-aldehyde that a straightforward analysis using spectrophotometry has been developed. The reagent 1,2-di-(4-pyridyl)ethylene was selected for the process due to its ability to react with ozone in minimal quantities, resulting in the form-ation of pyridine-4-aldehyde. Additionally, this reagent is soluble in water and can be easily detected using a modified version of 3-methyl-2-benzothiazolinone hydrazone method [31,32].

EXPERIMENTAL

Theoretical background: To order to determine precisely the electron injection into a titanium oxide (TiO_2) surface from selected 1,2-di-(4-pyridyl)ethylene derivatives, a robust theoretical approach is suggested. The proposed theoretical framework, which is deemed very dependable, is established on a comprehensive examination of the electrochemical characteristics of the studied dyes in their excited state. The change in free energy due to electron injection is reported in eV.

$$\Delta G^{inject} = E_{ox}^{dye*} - E_{CB}^{TiO_2} \quad (1)$$

where E_{ox}^{dye*} and $E_{CB}^{TiO_2}$ refer respectively, the oxidation potential and conduction band the dye's excited state's energy [33]. These precise determination for $E_{CB}^{TiO_2}$ is relatively long since the energy of the TiO_2 conduction band is dependent on the pH of the solution and the surface conditions. Therefore, based on this reported the readings of the various materials, we used $E_{CB}^{TiO_2} = 4.0$ eV [34]. The presented value has been determined by experimental methods and is based on the theoretical assumption that aqueous redox electrolytes, which maintain a constant pH, are in contact with the semiconductor. This model, which is based on the measurement of E_{ox}^{dye*} can evaluate the injection of electrons through a unrelaxed excited state [35]. The oxidation potential in an excited state for the reaction technique is obtained using the inter molecular charge transfer (ICT) generated by photons (λ_{max}^{ICT}) and the ground-state redox potential (E_{ox}^{dye*}).

$$E_{ox}^{dye*} = E_{ox}^{dye} - \lambda_{max}^{ICT} \quad (2)$$

If, λ_{max}^{ICT} is intermolecular charge transfer energy.

An effectiveness of DSSC is determined by the efficiency with which these dyes operate in reaction regard incident light. To maximize the reaction of photocurrent, the values must be as much as possible in accordance with dyes light harvesting efficiency (LHE). Using this formula, the light harvesting efficiency (LHE) was calculated as follows:

$$LHE = 1 - 10^{-f} \quad (3)$$

where f is the dye's oscillator strength.

Since electrons are injected into the conduction band from the LUMO (E_{CB}) of the semi-conductor TiO_2, the energy of the dye's LUMO (E_{LUMO}) my be utilized to calculate the open-circuit photo voltage V_{oc} (eV) [36].

$$V_{oc} = E_{LUMO} - E_{CB} \quad (4)$$

The electron coupling constant $|V_{RP}|$ is obtained from ΔG^{inject} using eqn. 5 [37]:

$$\left| V_{RP} \right| = \frac{\Delta G^{inject}}{2} \quad (5)$$

Computational method: In present study, 1,2-di-(4-pyridyl)ethylene sensitizers extensively initial vacuum-based calculations for the geometry optimization and electrical structure with use of the 6-311++G(d,p) basis set with the B3LYP functional. In three solvents, *viz.* dimethyl formamide (DMF), dichloromethane (DCM) and tetrahydrofuran (TFA), 1,2-di-(4-pyridyl)ethylene sensitizers were investigated. The ground state geometries of the sensitizers were developed using the polarized continuum model (PCM) using a bigger basis set 6-311++G(d,p) and each stationary point was verified with precise energy lowest frequency calculations performed at the same level. Calculations for the minimum frequency of energy were done the same studies. The software utilized for this computation was Gaussian 09 [38]. Density functional theory using the Lee-Yang-Parr functional and Becke's three parameters functional (B3LYP) was utilized tooptimize the ground state of the dyes structurally in the gas phase with the 6-311++G (d,p) basis set [39-41]. Frequency calculations were performed to ensure that each optimized geometry is located at the global minimum of the potential energy surface, analogous to the procedure used for geometry determination. As demonstrated by Magyar and Tretiak [42], a significant portion of Hartree-Fock exchange is employed to define the charge transfer states in various donor-π-acceptor systems. A long-range (B3LYP) method analyzes interactions over extremely long distances by comparing short- and long-range exchange rates of 19% HF and 81% B88 [43-47]. In addition, the B3LYP can properly predict the absorption spectra of D-π-A molecules and is useful for establishing suitable excitation energies [48-51].

RESULTS AND DISCUSSION

Molecular orbitals: Herein, the rationale behind structural alterations in 1,2-di-(4-pyridyl)ethylene based photosensitized

dyes was explored in an effort to boost the electron injection efficiency of DSSCs. Theoretically, a wide range of novel structures can be examined and any variations are possible. In organic sensitizers, DBA (donor, bridge and acceptor) groups are often to show achieve higher effectiveness of intramolecular charge transfer under photo induced conditions. The transfer of this charge requires conjugation of the anchoring and donor groups. The 1,2-di-(4-pyridyl)ethylene derivatives and newly developed sensitizers that generate sufficient DBA (Fig. 1) are evaluated and reported in the present work. The flow of electrons may be observed in Fig. 2 as they transfer from the auxiliary donor (AD) to the acceptor (A). As a result of this finding, the photochemists will be able to develop dyes for dye-sensitized solar cells that are even more efficient.
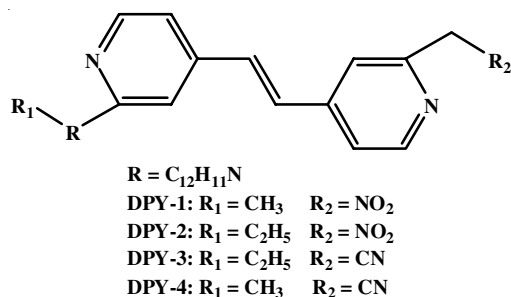

R = $C_{12}H_{11}N$
DPY-1: R_1 = CH_3 R_2 = NO_2
DPY-2: R_1 = C_2H_5 R_2 = NO_2
DPY-3: R_1 = C_2H_5 R_2 = CN
DPY-4: R_1 = CH_3 R_2 = CN
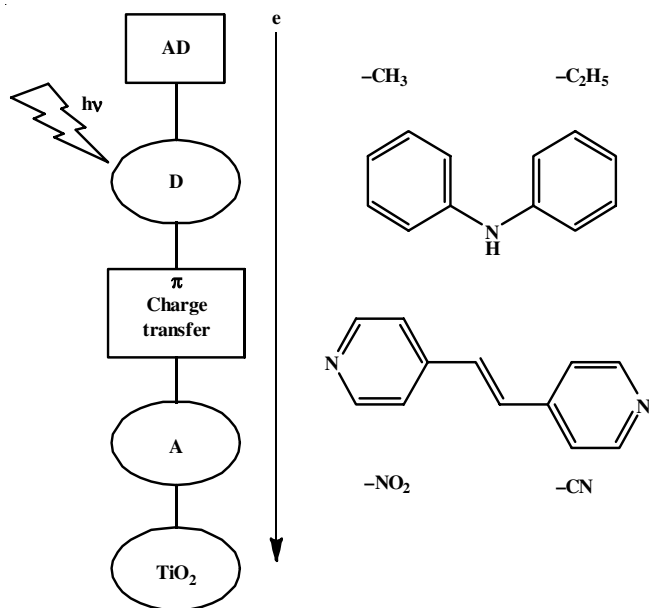
Fig. 1. Molecular structure of newly developed dyes

Fig. 2.   Different components of the 1,2-di-(4-pyridyl)ethylene AD-D-π-A system

A diphenyl amine moiety can be used as a spacer with various substituents acting as donors, while the terminal cyano (-C≡N) and nitro (-NO_2) groups act as acceptor units in these dyes. The electrolyte employed in DSSCs is typically system I^-/I_3^-. To order to understand the molecular structure and electronic distribution of these dyes, a molecular orbital (MO) investigation using the theory at the B3LYP/6-311++G (d,p) level was also performed. At DFT/B3LYP/6-311++G(d,p) level, Fig. 3 shows these HOMO as well as LUMO distribution pattern of 1,2-di-(4-pyridyl)ethylene based dyes. The results of the calculation of molecular orbital and energy gap are shown in Table-1. The electronic distribution of DPY, DPY-1, DPY-2, DPY-3 and DPY-4 molecules in gas phase is shown in Fig. 4a. When light is used to stimulate HOMO→LUMO excitation, the electronic charge is transferred from the acceptor component to the donor component with the π-spacer group, taking into account the molecular orbitals topology of DPY, DPY-1, DPY-2, DPY-3 and DPY-4. The molecule DPY-2 is mainly a 1,2-di-(4-pyridyl)ethylene acceptor and this molecule has a smaller energy gap. Additionally, three different solvents DMF, DCM and TFA media are the importance of electron injection-free energy is high in DPY-1. According to the result, a molecule DPY-1 has a nitro group and an ethyl group acting as auxiliary donor in the diphenylamine moiety indicates that it is a possible sensitizer. It appears to be a potential sensitizer in the 1,2-di-(4-pyridyl)ethylene group.

The process of spontaneous charge regeneration necessitates a higher negative energy level for the highest occupied molecular orbital (HOMO) compared to the reduction potential energy of the electrolyte (I^-/I_3^-), which was measured at -4.80 eV. In order for charge transfer to occur spontaneously from the dye-excited state to the conduction band of TiO_2, a greater energy level for the lowest unoccupied molecular orbital (LUMO) is required from the positive potential than the potential of TiO_2 (-4.0 eV).

Diagrams of the energy levels for this studied dyes HOMO and LUMO, the energy in the conduction band of TiO_2 (at -4.0 eV) and the redox potential energy of the solvents of the medium of gas phase, DMF, DCM and TFA are shown in Fig. 4. By employing the polarizable continuum model, the HOMO and LUMO energy levels of the dyes wre determined in the gas phase as well as in a number of solvents. A wide range of the dyes LUMOs are over the TiO_2 energy in the conduction band, while their HOMOs are just below the electrolyte's redox potential energy. This proves that TiO_2 and the spontaneous charge transfer and regeneration are compatible. Furthermore, it has been observed that when the parent compound 1,2-di-(4-

TABLE-1
MOLECULAR ORBITAL AND ENERGY GAP VALUES OF DYES (eV) AT B3LYP/6-311++G (d,p) LEVEL OF THEORY

Dye	Gas phase			DMF			DCM			TFA		
	HOMO	LUMO	E_{gap}	HOMO	LUMO	E_{gap}	HOMO	LUMO	E_{gap}	HOMO	LUMO	E_{gap}
DPY	-6.40071	-2.9604	3.4404	-6.3452	-2.9010	3.4442	-6.3498	-2.9054	3.4444	-6.3509	-2.9067	3.4442
DPY-1	-6.0353	-3.4366	2.5987	-5.9330	-3.4118	2.5216	-5.9373	-3.4025	2.5348	-5.9387	-3.4006	2.5380
DPY-2	-6.0328	-3.4368	2.5960	-5.9313	-3.4118	2.5195	-5.9354	-3.4036	2.5318	-5.9368	-3.4017	2.5350
DPY-3	-6.0051	-3.2983	2.7067	-5.9281	-3.1234	2.8047	-5.9286	-3.1457	2.7829	-5.9291	-3.1514	2.7778
DPY-4	-6.0072	-3.2978	2.7095	-5.9302	-3.1236	2.8066	-5.9324	-3.1470	2.7854	-5.9332	-3.1527	2.7805
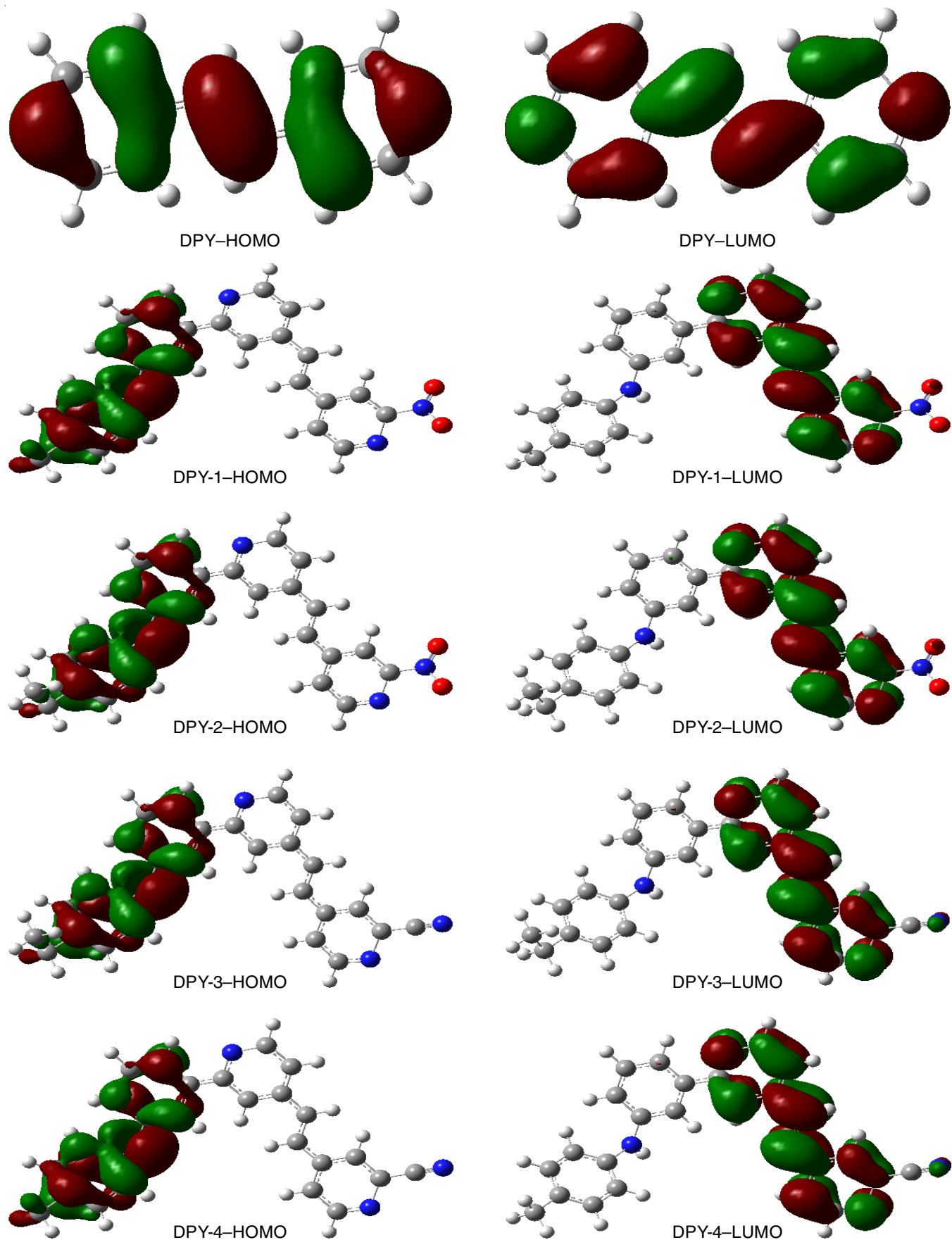
Fig. 3. 1,2-Di-(4-pyridyl)ethylene based dyes of HOMO and LUMO distribution pattern in gas phase by DFT/B3LYP/6-311++G(d,p) level of theory
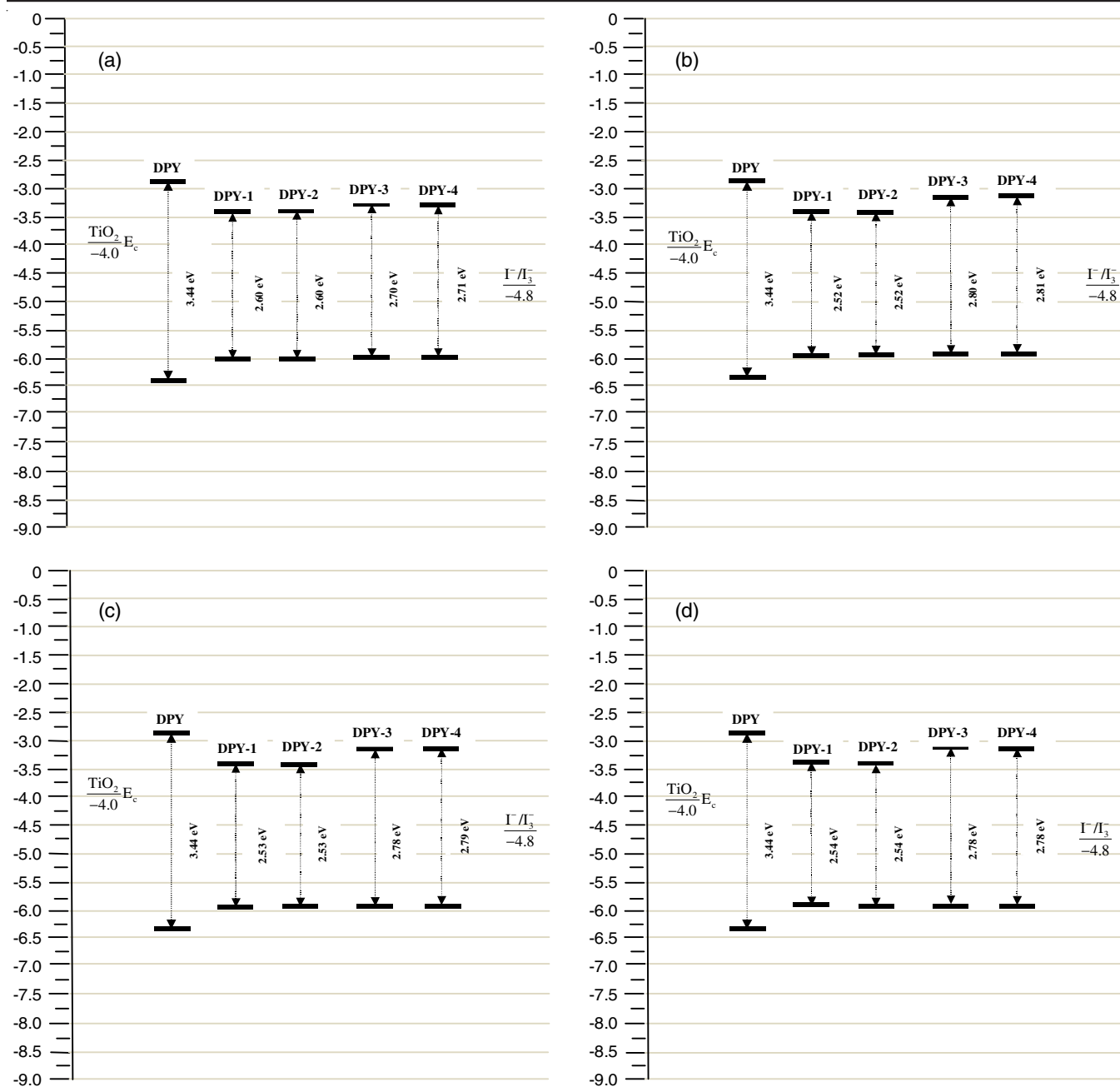
Fig. 4. Energy level diagram (E_{HOMO} and E_{LUMO}) of the 1,2-di-(4-pyridyl)ethylene based dyes in (a) gas phase, (b) DMF, (c) DCM and (d) TFA

pyridyl)ethylene (DPY) was utilized with DPA as a spacer, exhibits a comparatively elevated HOMO energy, while simultaneously displaying a reduced LUMO energy. The E_{gap} is thereby decreased in the dyes DPY to DPY-4. The studied 1,2-di-(4-pyridyl)ethylene derivatives (dyes) may clearly be seen in Fig. 4 to be suited as photosensitizers.

To help the DSSC dyes function more effectively and accurately, the co-absorbents enabled the bandgap at 400 nm in the dye-based UV spectrum by easily stimulating electrons into the TiO$_2$ layer (I^-/I_3^-) due to the continuous light absorption. For a conduction band match, a suitable LUMO and HOMO energy levels of sensitizers for the redox energy levels of the electrolyte and the TiO$_2$ electrode, respectively are required. The co-absorbents injecting electrons into the TiO$_2$ coating is

enhanced by higher LUMO values of DPY-2 (-3.4368 eV), DPY-1 (-3.4366 eV), DPY-3 (-3.2983 eV), DPY-4 (-3.2978 eV) and DPY (-2.9604 eV) in comparison with this ring of conduction edge of TiO$_2$ (-4.0 eV). A transfer of electrons from DPY-3, DPY-4, DPY-2, DPY-1 and DPY is reinforced by their lower HOMO values in comparison to the redox potential of the co-adsorbents. These levels are, successively, -6.0051 eV, -6.0072 eV, -6.0328 eV, -6.0353 eV and -6.4007 (-4.80 eV). All of the dyes in the three solvents follow the aforementioned pattern, as shown by continuous research and development. The orientation of the dye, together with its positive energy values, plays a pivotal role in facilitating charge transfer. The presence of these characteristics will facilitate the injection of electrons into TiO$_2$ and inhibit the rapid propagation of electrons from

TiO$_2$ for the oxidized dye, particularly in instances when power conversion efficiency (PCE) is relatively low. To ensure efficient energy transfer, it is advisable to place the HOMO of the dyes away from the surface of TiO$_2$. This is because the carbocation position in that region of the molecule lacks electrons. Those LUMO must be close to the TiO$_2$ surface the HOMO must pass the LUMO its intramolecular electrical charge following the excitation of photons. The provided information elucidates the presence of LUMO energies in the examined dyes, which closely align with the energy of the TiO2 surface. Additionally, the HOMO energies of the derivatives, namely 1,2-di-(4-pyridyl)-ethylene, are significantly far from the energy of TiO$_2$ surface. This observation suggests that these dyes have the potential to serve as effective light sensitizers for DSSC applications.

For a dye sensitizer to perform optimally in DSSC, it is essential that the energy levels of both its LUMO and HOMO are accurately aligned. The energy levels of the electrical conductor's band in the TiO$_2$ electrode should be comparable to the redox potential of the electrolyte. To achieve efficient electron injection, it is necessary for the excited state to possess a higher energy level and a lower electrochemical potential in comparison to the conduction band of TiO$_2$. It finds out that 1,2-di-(4-pyridyl)ethylene with -NO$_2$ acceptor and -C$_2$H$_5$ donor (DPY-2) has a smaller E$_{gap}$. Moreover, it can be observed that an increase in the polarity of the solvent leads to a decrease in the value of E$_{gap}$, however, the energy gap for DPY-2 decreases when it is dissolved in DMF.

For the dye cation to be restored to TiO$_2$ and acquire a more positive oxidation potential, it must be at a lower energy level than the redox electrolyte used after photoinduced electron injection. Since the carbocation site of the dyes will not contain any electrons, the HOMO should be placed distant from the TiO$_2$ surface for efficient energy conversion.

Optical properties: The UV-Vis absorption spectra of all the five dyes (Fig. 5) were simulated at the DFT/B3LYP/6-311++G (d,p) level for these singlet-singlet transitions in the gas phase and in these three different solvents to gain insight into the dyes' optical quality and electrical transition. The determined oscillator strength and wavelength among the sensitized dyes in this gas phase and three solvents are displayed in Table-2.
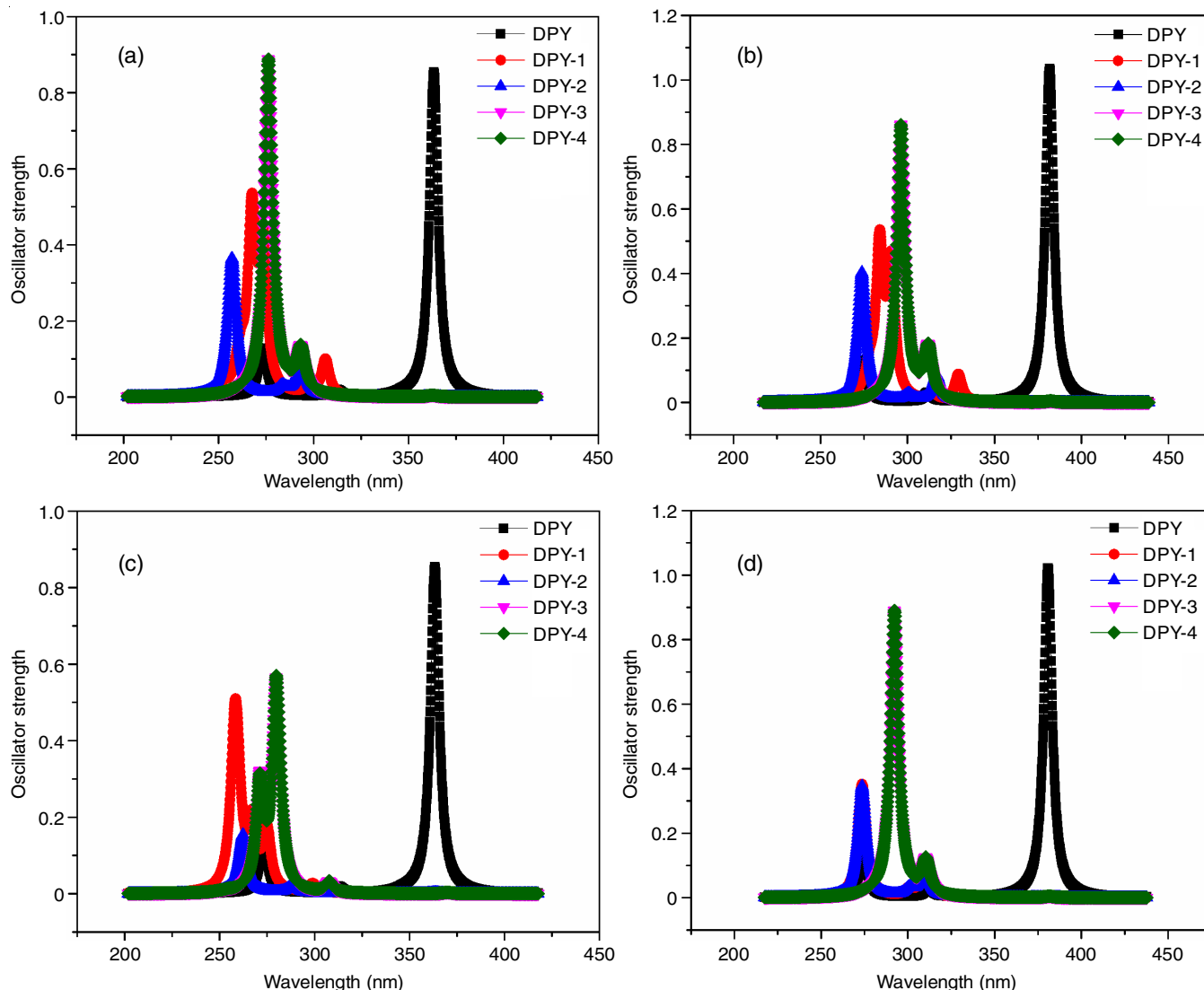

Fig. 5. Calculated dyes UV-visible absorption spectra (a) gas phase, (b) DMF, (c) DCM, (d) TFA by DFT/B3LYP/6-311+G(d,p) level of theory

TABLE-2
LIGHT HARVESTING EFFICIENCY (LHE) AND AVERAGE LIGHT HARVESTING EFFICIENCY (LHE_{avg}),
OSCILLATOR STRENGTH (f), ABSORPTION SPECTRA (λ_{max}) OF DYES AT B3LYP/6-311++G(d,p) LEVEL OF THEORY

Dye	λ_{max}	f	LHE	LHE_{avg}	λ_{max}	f	LHE	LHE_{avg}
	Gas phase				DMF			
DPY	347.02	0.0026	0.0060	0.0216	326.41	0.0035	0.0080	0.0363
	312.50	0.0164	0.0371		311.83	0.0290	0.0646	
DPY-1	441.33	0.0228	0.0511	0.1736	462.71	0.0838	0.1755	0.1119
	401.08	0.1525	0.2961		438.96	0.0215	0.0483	
DPY-2	441.44	0.0228	0.0511	0.1745	462.68	0.0838	0.1755	0.1119
	401.10	0.1536	0.2979		439.05	0.0215	0.0483	
DPY-3	386.91	0.1164	0.2351	0.4771	395.86	0.8572	0.8611	0.4345
	383.94	0.4673	0.6590		374.91	0.0034	0.0078	
DPY-4	386.89	0.1126	0.2284	0.4476	395.83	0.8568	0.8609	0.4344
	383.82	0.4772	0.6667		374.72	0.0034	0.0078	
	DCM				TFA			
DPY	329.40	0.0035	0.0080	0.0357	330.12	0.0034	0.0078	0.0349
	312.08	0.0284	0.0633		312.11	0.0278	0.0620	
DPY-1	454.12	0.0946	0.1957	0.1229	452.02	0.0954	0.1972	0.1239
	438.88	0.0223	0.0501		438.78	0.0225	0.0505	
DPY-2	454.17	0.0947	0.1959	0.1230	452.08	0.0955	0.1974	0.1240
	439.08	0.0223	0.0501		438.99	0.0225	0.0505	
DPY-3	396.14	0.8860	0.8700	0.4389	395.74	0.8882	0.8706	0.4393
	376.28	0.0034	0.0078		376.55	0.0035	0.0080	
DPY-4	396.10	0.8859	0.8700	0.4389	395.71	0.8882	0.8706	0.4392
	376.01	0.0034	0.0078		376.27	0.0034	0.0078	

The sensitizer's perspective revolves around the concept that oscillator strength is a crucial factor that is directly linked to the efficiency of light harvesting [52]. According to Table-2, the DPY-4 system exhibits a strong oscillator and possesses the highest predicted light harvesting efficiency among the sensitizers investigated in this study. The simulated spectra obtained through theoretical analysis demonstrate that the spectra of all the 5 dyes exhibit similar spectral characteristics in relation to their respective wavelengths. The technique depicted below would subsequently be used to report the initial vertical excitation energy (ΔE) of the dyes DPY > DPY-4 > DPY-3 > DPY-1 > DPY-2. This also reflects the resulting bathochromic shift and transferring from DPY to DPY-2. The electronegative the electron donating groups containing heteroatoms produce a slight blue shift and lower oscillator intensity in the spectra of DPY-3 and DPY-4 compared to DPY.

Due to their ability to effectively change HOMO and LUMO values of structurally rearranged donor and acceptor groups, as well as π-conjugated spacers, compounds of the donor-π-acceptor (D-π-A) class have garnered significant attention in the scientific community in recent times. Based on the findings shown in Table 2, it can be inferred that the nature of substituent and the spacer group exert an influence on the maximum absorption of the dyes under investigation. Thus, DPY λ_{max} value is the shortest, which may be due to the fact that electron-donating groups increase E_{HOMO} and decrease E_{LUMO}. Ooyama *et al.* [53] reported the similar results in their spectral analysis based colours made from catechol acting to be DSSC sensitizers. The absorption peak of a particular acceptor in 1,2-di-(4-pyridyl)ethylene group moves to a longer wavelength in because of an electron-releasing group. As a result, DPY-2 has a higher maximum rate of absorption than other dyes.

Present study incorporates the design structures of 1,2-di-(4-pyridyl)-ethylene dye, encompassing the following features: (i) the spacer DPA serves to be the π-conjugated form (ii) alkyl and amine groupings act as a moiety that donates electrons and (iii) 1,2-di-(4-pyridyl)ethylene as the heterocyclic system with π-conjugation; and (iv) nitro and cyano groups act as a source of electrons. Every visible wavelength, as well as some near-infrared wavelengths, should normally be included in the photosensitizers' absorption spectrum [54]. Such compounds have a significant visible wavelength absorption area between 400-600 nm, particularly in solution. They are newly developed molecules because of the spacer DPA, which results in DPY to DPY molecular sizes greater than the fundamental dye 1,2-di-(4-pyridyl)ethylene molecule, 1,2-di-(4-pyridyl)-ethylene derivatives have been used by covering the base, a compact monolayer can form TiO_2 surface throughout the dye absorption process. Based on the aforementioned results, it may be claimed that the DPY–DPY-4 molecules, specifically DPY-1 and DPY-2, can be regarded as optimal co-adsorbents. Amounts of λ_{max}^{ICT} intramolecular charge transfer (ICT) are presented in Table-2 to determine the magnitude of the phenomenon in the dyes. It is clear from the data that addition of a DPA spacer to the 1,2-di-(4-pyridyl)ethylene moiety increases the ICT energy. The energy consumption of ICT, however, is not much influenced by the nature of the substituent.

Intramolecular charge transfer: The fundamental contribution of frontier molecular orbitals (FMOs) arises from the behavior shown by the dyes. Fig. 3 illustrates the spatial distribution of the HOMO and LUMO states for each colour. Due to the difference in electron distributions between the HOMO and LUMO patterns, the electronic transition of the π-π* types is correlated with those singlets of LUMOs and occupy the

lowest energy state, although their qualitative similarities cease there. In HOMOs, the conjugated spacer allows the electron sharing primarily between the electron donor and itself. In contrast, LUMOs are located on the π-conjugated spacer component as well as the electron acceptor groups, specifically nitro and cyano.

The transfer of charges between the acceptor/anchoring groups and the donor units within the molecular system occurs through the conjugated bridge. This charge transfer is observed in any D-π-A dye that undergoes electronic transformation from HOMO to LUMO, therefore, these HOMO-LUMO conversions are labelled as an π-π* ICT. The bonding of the anchoring groups (nitro and cyano) of the dyes to the LUMOs considerably enhanced the electron injection efficiencies by developing a strong electrical relate on the surface of TiO$_2$. The short-circuit current density (J$_{SC}$) also gradually rises as a result. Electronic injection free energy (ΔG^{inject}), open circuit photovoltage (V$_{OC}$), current density (J$_{SC}$) and light harvesting energy (LHE) are the main components to be considered when developing efficient DSSCs. These considerations also include the ground (E_{ox}^{dye}) and excited (E_{ox}^{dye*}) state oxidation potentials. Many studies have been done to improve these characteristics in order to maximize power conversion efficiency [55-57]. In all of these dyes, Koopman's theorem assumes that the oxidation potential in ground-state (E_{ox}^{dye}) is the negative E_{HOMO} [58]. Using eqn. 2, the values of E_{ox}^{dye*} were calculated and the values of the excited state's E_{ox}^{dye*} and ground state's E_{ox}^{dye} oxidation potentials of ground state are displayed in Table-3. It is evident that the order of all dyes in E_{ox}^{dye*} is DPY-3 < DPY-4 < DPY < DPY-2 < DPY-1. The results show that among the four dyes, DPY-3 is the most suitable oxidizing species, whereas DPY-1 is the least suitable one. The ΔG^{inject} values of the dyes under investigation were derived by utilizing eqn. 1 to predict the redox process. All of these factors indicate to the dye's spontaneous electron injection into TiO$_2$ through its negative charge. The results shown in Table-3 indicate the following order, which governs the calculations ΔG^{inject} as DPY-1 > DPY-2 > DPY > DPY-4 > DPY-3 in the gas phase and the arrangement of all solvents were DPY-1 > DPY-2 > DPY-4 > DPY-3 > DPY. Further, DPY-1 has the most significant ΔG^{inject} as long as DPY has the smallest value. The ΔG^{inject} values are affected by solvent and the negative values

in less polar solvents like DCM than in more polar solvents like TFA.

When shifting from DPY to DPY-1, we are able to determine the anodic shift of 0.3654 eV and 0.3982 eV of E_{ox}^{dye} and E_{ox}^{dye*} accordingly. On analyzing the oxidation potentials in the gas phase, it was observed that a cathodic shift of 0.0272 eV and 0.0252 eV occurred in the DPY to DPY-3 and DPY to DPY-4 transitions, respectively. It was observed that the introduction of the solvent resulted in an anodic shift, as evidenced by the comparison of the oxidation potentials in the gas phase and those in the presence of solvents. Both series, *i.e.* DPY→DPY-2→DPY-3 and DPY→DPY-1→DPY-2 →DPY-4→DPY-3, when observed both in the gas phase and in various solvents demonstrate a minor anodic shift.

The current density (J$_{SC}$) value is important for improving the light harvesting efficiency (LHE) that increases the effectiveness of DSSCs. An average values for LHE for the dyes are shown in Table-2. The spectral profiles of further simulated dyes are broadened in the sequence as DPY < DPY-1 < DPY-2 < DPY-3 < DPY-4. According to these results, systems using an alkyl a group that includes a donor and cyano group indicates acceptor can produce high LHE. If cyano group is the acceptor, LHE is lower for the dyes. The results readily indicates that the LHE value increases when the alkyl group in the diphenyl amine moiety is replaced by an amino substituent. According to these results, a system using an alkyl group indicates donor and a cyano group denotes acceptor can produce high LHE. If nitro group is the acceptor, LHE is lower for the dyes, which clearly show that the LHE value increases when alkyl group in diphenyl amine moiety is substituted by an amino substituent. The LHE values obtained for each dye exhibit in the range of 0.02-0.45, suggesting that all sensitizers generate a similar range of photocurrent (Table-3). The open circuit voltage (V$_{OC}$) was an essential component in the developement of DSSCs. The determined V$_{OC}$ levels among the dyes indicated that these amount for solar energy was converted into electricity (Table-4) [59,60]. It is obvious that the potential value for dyes under study ranges from 0.57 to 1.10 V. The studied dyes based on 1,2-di-(4-pyridyl)ethylene exhibit satisfactory values of V$_{OC}$, which facilitate enhanced electron injection from the excited lowest unoccupied molecular orbital (E$_{LUMO}$) into the condu-

TABLE-3
CALCULATED ABSORPTION SPECTRA λ_{max}, OXIDATION POTENTIAL (ΔG^{inject}),
INTRAMOLECULAR CHARGE TRANSFER ENERGY OF DYES AT B3LYP/6-311++G(d,p) THEORY

Dye	λ_{max}	λ_{max}^{ICT}	E_{ox}^{dye*}	ΔG^{inject}	λ_{max}	λ_{max}^{ICT}	E_{ox}^{dye*}	ΔG^{inject}
	Gas phase				DMF			
DPY	347.02	3.5729	2.8278	-1.1722	326.41	3.7985	2.5467	-1.4533
DPY-1	441.33	2.8093	3.2260	-0.7740	462.71	2.6795	3.2535	-0.7465
DPY-2	441.44	2.8086	3.2242	-0.7758	462.68	2.6797	3.2516	-0.7484
DPY-3	386.91	3.2045	2.8006	-1.1994	395.86	3.1320	2.7961	-1.2039
DPY-4	386.89	3.2047	2.8025	-1.1975	395.83	3.1322	2.7980	-1.2020
	DCM				TFA			
DPY	329.40	3.7640	2.5858	-1.4142	330.12	3.7558	2.5951	-1.4049
DPY-1	454.12	2.7302	3.2071	-0.7929	452.02	2.7429	3.1958	-0.8042
DPY-2	454.17	2.7299	3.2055	-0.7945	452.08	2.7425	3.1943	-0.8057
DPY-3	396.14	3.1298	2.7988	-1.2012	395.74	3.1329	2.7962	-1.2038
DPY-4	396.10	3.1301	2.8023	-1.1977	395.71	3.1332	2.8000	-1.2000

TABLE-4
ELECTRON COUPLING CONSTANTS ($|V_{RP}|$) AND OPEN-CIRCUIT PHOTO
VOLTAGE (eV) (V_{oc}) OF 1,2-DI-(4-PYRIDYL)ETHYLENE BASED DYES

Dye	Gas phase		DMF		DCM		TFA	
	$|V_{RP}|$	V_{oc}	$|V_{RP}|$	V_{oc}	$|V_{RP}|$	V_{oc}	$|V_{RP}|$	V_{oc}
DPY	0.59	1.04	0.73	1.10	0.71	1.09	0.70	1.09
DPY-1	0.39	0.56	0.37	0.59	0.40	0.60	0.40	0.60
DPY-2	0.39	0.56	0.37	0.59	0.40	0.60	0.40	0.60
DPY-3	0.60	0.70	0.60	0.88	0.60	0.85	0.60	0.85
DPY-4	0.60	0.70	0.60	0.88	0.60	0.85	0.60	0.85

ction band of TiO_2. This suggests that these dyes are suitable for the utilization in the advancement of dye-sensitized solar cells (DSSCs). The coupling constant ($|V_{RP}|$) determines the rate at which the electrons are injected into the semiconductor surface by the organic dyes. A greater electron injection rate will result from a higher electron-coupling constant (Table-4). According to Irfan *et al.* [61], the utilization of DFT was employed to modify the composition of materials utilized in solar cells. The findings suggested that an increase in the donor portion of the sensitizer, characterized by a higher concentration of activating groups, led to an occurrence of ΔG^{inject}. Conversely, an increase in the acceptor portion of the sensitizer, characterized by a higher concentration of deactivating groups, resulted in an increase in V_{RP}. In present work, it was found when the donor moiety of DPY-1 containing -CH_3, while the acceptor portion contains -NO_2 group have high V_{RP}. Similar to DPY-3, which has high V_{RP} values and a donor that contains more activating -C_2H_5 groups and deactivating -CN groups. Therefore, the frequency of electron injection in these dyes is significant. A low value of voltage reduction potential (V_{RP}) is likewise observed in the case of DPY-1, indicating a comparatively delayed electron injection process inside this particular system. The photocurrent density under short circuit conditions was calculated by J_{SC} using the yield of electron injection, which is dependent on the sensitizer's quantitative as well as qualitative absorption properties and on an effective positioning of the sensitizers LUMO level along with the semiconductor. In 1,2-di-(4-pyridyl)ethylene derivatives, the value of dye DPY-3 is comparatively higher in comparable gaseous and solvents forms. As a result, a J_{SC} having a high short-circuit current density may be produced. Excessive regeneration energy, which also results in a lower V_{oc} reduces the effectiveness of converting solar energy.

Conclusion

This study discusses the properties of electrical as well as optical absorption of particular 1,2-di-(4-pyridyl)ethylene based organic dyes with π-conjugated spacers (DPA) to assess their potential applications in DSSCs. These new compounds contain diphenylamine as a spacer and a component of an electron donor generated from alkyl (methyl and ethyl) groups. The cyano molecule or nitro molecular group functions acting as anchor and acceptor for 1,2-di-(4-pyridyl)ethylene group. For these dyes, the gas phase as well as in three distinct solvents, computed E_{HOMO} and E_{LUMO} values were calculated. The performance of sensitizers in DSSC systems using relevant choose electronic and optical properties and light harvesting efficiency

was also investigated. An electron acceptor group in 1,2-di-(4-pyridyl)ethylene moiety of the molecule and the electron donoating group in the diphenylamine molecule also improved the ΔG^{inject} and LHE of the novel photo-sensitizers. Based on the estimated ΔG^{inject}, V_{RP} and V_{OC} values of these dyes possess a significant potential for usage in DSSC photo-sensitizers. The thermodynamic and kinetic properties of the sensitizers show that these systems could be used in an efficient way of photo-sensitizers for DSSCs. All of these suggested dyes had strong electron injection driving forces due to their greater short-circuit current density. Thus, the newly developed metal-free organic dyes offer some promising alternatives that might improved the power conversion efficiency of the DSSCs.

CONFLICT OF INTEREST

The authors declare that there is no conflict of interests regarding the publication of this article.

REFERENCES

1. W. Strielkowski, L. Civín, E. Tarkhanova, M. Tvaronaviciene and Y. Petrenko, *Energies*, **14**, 8240 (2021);
https://doi.org/10.3390/en14248240
2. N. Panwar, S. Kaushik and S. Kothari, *Renew. Sustain. Energy Rev.*, **15**, 1513 (2011);
https://doi.org/10.1016/j.rser.2010.11.037
3. M.A. Hasan and K. Sumathy, *Renew. Sustain. Energy Rev.*, **14**, 1845 (2010);
https://doi.org/10.1016/j.rser.2010.03.011
4. M. Gratzel, *J. Photochem. Photobiol. Chem.*, **164**, 3 (2004);
https://doi.org/10.1016/j.jphotochem.2004.02.023
5. J.M. Pearce, *Futures*, **34**, 663 (2002);
https://doi.org/10.1016/S0016-3287(02)00008-3
6. H. Hoppe and N.S. Sariciftci, *J. Mater. Res.*, **19**, 1924 (2004);
https://doi.org/10.1557/JMR.2004.0252
7. S. Gunes, H. Neugebauer and N.S. Sariciftci, *Chem. Rev.*, **107**, 1324 (2007);
https://doi.org/10.1021/cr050149z
8. B. O'regan and M. Gratzel, *Nature*, **353**, 737 (1991);
https://doi.org/10.1038/353737a0
9. F. Gao, Y. Wang, D. Shi, J. Zhang, M. Wang, R. Humphry-Baker, X. Jing, P. Wang, S.M. Zakeeruddin and M. Grätzel, *J. Am. Chem. Soc.*, **130**, 10720 (2008);
https://doi.org/10.1021/ja801942j
10. K. Sharma, V. Sharma and S.S. Sharma, *Nanoscale Res. Lett.*, **13**, 381 (2018);
https://doi.org/10.1186/s11671-018-2760-6
11. J. Gong, J. Liang and K. Sumathy, *Renew. Sustain. Energy Rev.*, **16**, 5848 (2012);
https://doi.org/10.1016/j.rser.2012.04.044
12. B. Chen, S. Ma, F. Zapata, E.B. Lobkovsky and J. Yang, *Inorg. Chem.*, **45**, 5718 (2006);
https://doi.org/10.1021/ic060437t
13. D.N. Dybtsev, M.P. Yutkin, E.V. Peresypkina, A.V. Virovets, C. Serre, G. Férey and V.P. Fedin, *Inorg. Chem.*, **46**, 6843 (2007);
https://doi.org/10.1021/ic7009226

14. N.L. Toh, M. Nagarathinam and J.J. Vittal, *Angew. Chem. Int. Ed.*, **44**, 2237 (2005);
https://doi.org/10.1002/anie.200462673

15. T.K. Maji, K. Uemura, H.-C. Chang, R. Matsuda and S. Kitagawa, *Angew. Chem. Int. Ed.*, **43**, 3269 (2004);
https://doi.org/10.1002/anie.200453923

16. G.S. Papaefstathiou, Z. Zhong, L. Geng and L.R. MacGillivray, *J. Am. Chem. Soc.*, **126**, 9158 (2004);
https://doi.org/10.1021/ja047819n

17. M. Wang, Y.-R. Zheng, K. Ghosh and P.J. Stang, *J. Am. Chem. Soc.*, **132**, 6282 (2010);
https://doi.org/10.1021/ja100889h

18. L. Ma, O.R. Evans, B.M. Foxman and W. Lin, *Inorg. Chem.*, **38**, 5837 (1999);
https://doi.org/10.1021/ic990429v

19. T.M. Reineke, M. Eddaoudi, M. Fehr, D. Kelley and O.M. Yaghi, *J. Am. Chem. Soc.*, **121**, 1651 (1999);
https://doi.org/10.1021/ja983577d

20. Z.S. Bai, J. Xu, T. Okamura, M.-S. Chen, W.-Y. Sun and N. Ueyama, *Dalton Trans.*, **14**, 2528 (2009);
https://doi.org/10.1039/b816205k

21. S.V. Eliseeva and J.-C.G. Bünzli, *New J. Chem.*, **35**, 1165 (2011);
https://doi.org/10.1039/c0nj00969e

22. L. Sorace, C. Benelli and D. Gatteschi, *Chem. Soc. Rev.*, **40**, 3092 (2011);
https://doi.org/10.1039/c0cs00185f

23. S. Mohapatra, S. Adhikari, H. Riju and T.K. Maji, *Inorg. Chem.*, **51**, 4891 (2012);
https://doi.org/10.1021/ic300237e

24. S.I. Weissman, *J. Chem. Phys.*, **10**, 214 (1942);
https://doi.org/10.1063/1.1723709

25. G.A. Crosby, R.E. Whan and R.M. Alire, *J. Chem. Phys.*, **34**, 743 (1961);
https://doi.org/10.1063/1.1731670

26. L. Armelao, S. Quici, F. Barigelletti, G. Accorsi, G. Bottaro, M. Cavazzini and E. Tondello, *Coord. Chem. Rev.*, **254**, 487 (2010);
https://doi.org/10.1016/j.ccr.2009.07.025

27. P.A. Tanner and C.-K. Duan, *Coord. Chem. Rev.*, **254**, 3026 (2010);
https://doi.org/10.1016/j.ccr.2010.05.009

28. D. Parker and J.A.G. Williams, *J. Chem. Soc., Dalton Trans.*, 3613 (1996);
https://doi.org/10.1039/dt9960003613

29. P. Gawryszewska, J. Sokolnicki and J. Legendziewicz, *Coord. Chem. Rev.*, **249**, 2489 (2005);
https://doi.org/10.1016/j.ccr.2005.06.021

30. N. Dannenbauer, P.R. Matthes, T.P. Scheller, J. Nitsch, S.H. Zottnick, M.S. Gernert, A. Steffen, C. Lambert and K. Müller-Buschbaum, *Inorg. Chem.*, **55**, 7396 (2016);
https://doi.org/10.1021/acs.inorgchem.6b00447

31. T.R. Hauser and D.W. Bradley, *Anal. Chem.*, **38**, 1529 (1966);
https://doi.org/10.1021/ac60243a018

32. E. Sawicki, T.R. Hauser, T.W. Stanley and W. Elbert, *Anal. Chem.*, **33**, 93 (1961);
https://doi.org/10.1021/ac60169a028

33. R. Katoh, A. Furube, T. Yoshihara, K. Hara, G. Fujihashi, S. Takano, S. Murata, H. Arakawa and M.J. Tachiya, *J. Phys. Chem. B*, **108**, 4818 (2004);
https://doi.org/10.1021/jp031260g

34. J.B. Asbury, Y.-Q. Wang, E. Hao, H.N. Ghosh and T. Lian, *Res. Chem. Intermed.*, **27**, 393 (2001);
https://doi.org/10.1163/156856701104202255

35. A. Hagfeldt and M. Graetzel, *Chem. Rev.*, **95**, 49 (1995);
https://doi.org/10.1021/cr00033a003

36. Z.-G. Zhang, J. Min, S. Zhang, J. Zhang, M. Zhang and Y. Li, *Chem. Commun.*, **47**, 9474 (2011);
https://doi.org/10.1039/c1cc13477a

37. J.O. Odey, H. Louis, J.A. Agwupuye, Y.L. Moshood, E.A. Bisong and O.I. Brown, *J. Mol. Struct.*, **1241**, 130615 (2021);
https://doi.org/10.1016/j.molstruc.2021.130615

38. M.J. Frisch, G.W. Trucks, H.B. Schlegel, G.E. Scuseria, M.A. Robb, J.R. Cheeseman, G. Scalmani, V. Barone, G.A. Petersson, H. Nakatsuji, X. Li, M. Caricato, A. Marenich, J. Bloino, B.G. Janesko, R. Gomperts, B. Mennucci, H.P. Hratchian, J.V. Ortiz, A.F. Izmaylov, J.L. Sonnenberg, D. Williams-Young, F. Ding, F. Lipparini, F. Egidi, J. Goings, B. Peng, A. Petrone, T. Henderson, D. Ranasinghe, V.G. Zakrzewski, J. Gao, N. Rega, G. Zheng, W. Liang, M. Hada, M. Ehara, K. Toyota, R. Fukuda, J. Hasegawa, M. Ishida, T. Nakajima, Y. Honda, O. Kitao, H. Nakai, T. Vreven, K. Throssell, J.A. Montgomery, Jr., J.E. Peralta, F. Ogliaro, M. Bearpark, J.J. Heyd, E. Brothers, K.N. Kudin, V.N. Staroverov, T. Keith, R. Kobayashi, J. Normand, K. Raghavachari, A. Rendell, J.C. Burant, S.S. Iyengar, J. Tomasi, M. Cossi, J.M. Millam, M. Klene, C. Adamo, R. Cammi, J.W. Ochterski, R.L. Martin, K. Morokuma, O. Farkas, J.B. Foresman and D.J. Fox, Gaussian, Inc., Wallingford CT (2016).

39. A.D. Becke, *J. Chem. Phys.*, **98**, 1372 (1993);
https://doi.org/10.1063/1.464304

40. A.D. Becke, *Phys. Rev. A Gen. Phys.*, **38**, 3098 (1988);
https://doi.org/10.1103/PhysRevA.38.3098

41. C. Lee, W. Yang and R.G. Parr, *Rev. Bus.*, **37**, 785 (1988).

42. R.J. Magyar and S. Tretiak, *J. Chem. Theory Comput.*, **3**, 976 (2007);
https://doi.org/10.1021/ct600282k

43. T. Yanai, D.P. Tew and N.C. Handy, *Chem. Phys. Lett.*, **393**, 51 (2004);
https://doi.org/10.1016/j.cplett.2004.06.011

44. Y. Xue, L. An, Y. Zheng, L. Zhang, X. Gong, Y. Qian and Y. Liu, *Comput. Theor. Chem.*, **981**, 90 (2012);
https://doi.org/10.1016/j.comptc.2011.11.050

45. A.W. Lange, M.A. Rohrdanz and J.M. Herbert, *J. Phys. Chem. B*, **112**, 6304 (2008);
https://doi.org/10.1021/jp802058k

46. M.A. Rohrdanz and J.M. Herbert, *J. Chem. Phys.*, **129**, 34107 (2008);
https://doi.org/10.1063/1.2954017

47. J. Toulouse, F. Colonna and A. Savin, *J. Chem. Phys.*, **122**, 14110 (2005);
https://doi.org/10.1063/1.1824896

48. J. Preat, *J. Phys. Chem. C*, **114**, 16716 (2010);
https://doi.org/10.1021/jp1050035

49. B. Camino, M. De-La-Pierre and A.M. Ferrari, *J. Mol. Struct.*, **1046**, 116 (2013);
https://doi.org/10.1016/j.molstruc.2013.04.010

50. A. Irfan, R. Jin, A.G. Al-Sehemi and A.M. Asiri, *Spectrochim. Acta A Mol. Biomol. Spectrosc.*, **110**, 60 (2013);
https://doi.org/10.1016/j.saa.2013.02.045

51. A. Fitri, A.T. Benjelloun, M. Benzakour, M. Mcharfi, M. Hamidi and M. Bouachrine, *Spectrochim. Acta A Mol. Biomol. Spectrosc.*, **124**, 646 (2014);
https://doi.org/10.1016/j.saa.2014.01.052

52. X. Li, P. Song, D. Zhao and Y. Li, *Materials*, **13**, 4834 (2020);
https://doi.org/10.3390/ma13214834

53. Y. Ooyama, M. Kanda, K. Uenaka and J. Ohshita, *ChemPhysChem*, **16**, 3049 (2015);
https://doi.org/10.1002/cphc.201500419

54. K. Moneer, *J. Glob. Pharma Technol.*, **12**, 206 (2017).

55. K. Kakiage, H. Osada, Y. Aoyama, T. Yano, K. Oya, S. Iwamoto, J. Fujisawa and M. Hanaya, *Sci. Rep.*, **6**, 35888 (2016);
https://doi.org/10.1038/srep35888

56. L. Etgar, G. Schuchardt, D. Costenaro, F. Carniato, S.M. Zakeeruddin, C. Bisio, M.K. Nazeeruddin, L. Marchese and M. Graetzel, *J. Mater. Chem. A Mater. Energy Sustain.*, **1**, 10142 (2013);
https://doi.org/10.1039/c3ta11436h

57. Z. Liu, L. Krückemeier, B. Krogmeier, B. Klingebiel, J.A. Márquez, S. Levcenko, S. Öz, S. Mathur, U. Rau, T. Unold and T. Kirchartz, *ACS Energy Lett.*, **4**, 110 (2019);
https://doi.org/10.1021/acsenergylett.8b01906

58. R.G. Pearson, *Inorg. Chem.*, **27**, 734 (1988);
https://doi.org/10.1021/ic00277a030

59. H. Wang, Y. Li, P. Song, F. Ma and Q. Wang, *Mol. Phys.*, **114**, 3518 (2016);
https://doi.org/10.1080/00268976.2016.1244357

60. W. Sang-aroon, S. Saekow and V. Amornkitbamrung, *J. Photochem. Photobiol. Chem.*, **236**, 35 (2012);
https://doi.org/10.1016/j.jphotochem.2012.03.014

61. A. Irfan, S. Muhammad, A.G. Al-Sehemi, M.S. Al-Assiri and A. Kalam, *Int. J. Electrochem. Sci.*, **10**, 3600 (2015);
https://doi.org/10.1016/S1452-3981(23)06564-1